

Reliable tree height estimation in agroforestry and reforestation system using Airborne Laser Scanning (ALS)

Tiodionwa Abdoulaye Ouattara^{1,2,*}, N'zi Daniel Koua^{1,2}, Nina Gueulou², Yao Henri-Michel Ella³, Patrick Muziga⁴, Kouamé Kissi Patrice Adayé²

¹ National Polytechnic Institute Félix Houphouët-Boigny (INP-HB), BP 2661, Yamoussoukro 2661, Ivory Coast

² AGROMAP, Abidjan Angré 7eme tranche, Cocody 22, Ivory Coast

³ Ivorian Office of Parks and Reserves (OIPR), Cocody 22, Ivory Coast

⁴ Charis Unmanned Aerial Solutions (CHARIS-UAS), Abidjan 30, Ivory Coast

* Corresponding author: Tiodionwa Abdoulaye Ouattara, tiodionwa.ouattara@inphb.ci

CITATION

Ouattara TA, Koua ND, Gueulou N, et al. Reliable tree height estimation in agroforestry and reforestation system using Airborne Laser Scanning (ALS). *Sustainable Forestry*. 2025; 8(1): 11725. <https://doi.org/10.24294/sf11725>

ARTICLE INFO

Received: 30 April 2025

Accepted: 4 June 2025

Available online: 13 June 2025

COPYRIGHT



Copyright © 2025 by author(s).

Sustainable Forestry is published by EnPress Publisher, LLC. This work is licensed under the Creative Commons Attribution (CC BY) license.

<https://creativecommons.org/licenses/by/4.0/>

Abstract: In Côte d'Ivoire, the government and its development partners have implemented a national strategy to promote agroforestry and reforestation systems as a means to combat deforestation, primarily driven by agricultural expansion, and to increase national forest cover to 20% by 2045. However, the assessment of these systems through traditional field-based methods remains labor-intensive and time-consuming, particularly for the measurement of dendrometric parameters such as tree height. This study introduces a remote sensing approach combining drone-based Airborne Laser Scanning (ALS) with ground-based measurements to enhance the efficiency and accuracy of tree height estimation in agroforestry and reforestation contexts. The methodology involved two main stages: first, the collection of floristic and dendrometric data, including tree height measured with a laser rangefinder, across eight (8) agroforestry and reforestation plots; second, the acquisition of ALS data using Mavic 3E and Matrice 300 drones equipped with LiDAR sensors to generate digital canopy models for tree height estimation and associated error analysis. Floristic analysis identified 506 individual trees belonging to 27 genera and 18 families. Tree height measurements indicated that reforestation plots hosted the tallest trees (ranging from 8 to 16 m on average), while cocoa-based agroforestry plots featured shorter trees, with average heights between 4 and 7 m. A comparative analysis between ground-based and LiDAR-derived tree heights showed a strong correlation ($R^2 = 0.71$; $r = 0.84$; RMSE = 2.24 m; MAE = 1.67 m; RMSE = 2.2430 m and MAE = 1.6722 m). However, a stratified analysis revealed substantial variation in estimation accuracy, with higher performance observed in agroforestry plots ($R^2 = 0.82$; RMSE = 2.21 m and MAE = 1.43 m). These findings underscore the potential of Airborne Laser Scanning as an effective tool for the rapid and reliable estimation of tree height in heterogeneous agroforestry and reforestation systems.

Keywords: drone; LiDAR; ALS; agroforestry; reforestation; Côte d'Ivoire

1. Introduction

Forests cover around 31% of the land surface and play a critical role in maintaining global ecological balance [1]. They harbor around 80% of terrestrial biodiversity, deliver essential ecosystem services (including climate regulation and water purification), and serve as major carbon sinks by sequestering atmospheric carbon dioxide (CO₂), thereby mitigating the impact of climate change [1]. Nevertheless, deforestation, driven predominantly by agricultural expansion, logging, and urban development, constitutes a significant global threat. It is estimated that nearly 10 million hectares of forest are lost annually, equivalent to one soccer field

every six seconds [1,2]. In West Africa, Côte d'Ivoire exemplifies a country that has experienced rapid and severe forest loss within a relatively short timeframe. National forest cover declined from 16 million hectares in 1900 to 7.9 million hectares by 1986 [3]. This downward trend persisted, with forest area shrinking to 5.1 million hectares in 2000 and further to 3.4 million hectares by 2015, representing merely 11% of the national territory [3]. The loss is therefore more than 75% and has continued at a rate of around 110,000 hectares per year since 2015. A qualitative analysis of deforestation drivers identified agriculture (62%), logging (18%), and infrastructure expansion (10%) as the primary direct causes of forest loss [4]. Among these, cocoa cultivation, the country's principal export crop, is directly implicated in the ongoing deforestation crisis. Today, the global cocoa value chain faces mounting challenges related to economic viability, social equity, and environmental sustainability. In response, a number of sustainability initiatives, such as the Rainforest Alliance, Fairtrade, ARS 1000 Sustainable Cocoa Standard, and the EU Regulation on deforestation-free products, are being developed and implemented throughout the cocoa production zone. These programs aim to encourage agroforestry practices by promoting tree planting within cocoa plantations [5]. Traditionally, tree growth has been monitored through ground-based surveys to assess survival rates, increases in tree diameter and height, and biomass carbon sequestration. However, these field-based campaigns require substantial human and financial resources over extended periods and are often subject to measurement errors. As a result, the integration of geospatial technologies offering greater efficiency and reduced labor intensity has become increasingly necessary for such assessments. Among these technologies, Light Detection and Ranging (LiDAR) has gained recognition for its capability to characterize forest canopy structure with high accuracy [6 – 8]. Key advantages of LiDAR include high sampling density, fine spatial resolution, wide spatial coverage, the ability to penetrate upper canopy layers, and precise geolocation capabilities, making it an indispensable tool for the evaluation of vegetation structure and biomass [9,10]. LiDAR enables detailed 3D modeling of trees, providing accurate visualizations [11]. Numerous studies have demonstrated the relevance of this LiDAR in sustainable forest management and ecological research. In Brazil, Oliveira et al. [12] used Airborne Laser Scanning data as reference data to calibrate the Landsat satellite to improve estimates of structural parameters of Amazonian vegetation. In Costa Rica, Ferraz et al. [13] used the same technology and field inventory data to improve forest carbon stock estimates. Other studies have contributed significantly to the improvement of 3D tree modeling techniques, focusing on precision, automation, and efficiency. For instance, Tarsha Kurdi et al. [14] introduced an innovative approach for accurately calculating the upper biomass volume of individual trees using LiDAR data. Also, he proposes an approach to automatically model tree trunk geometry from point cloud data obtained by laser scanning [15]. In light of the challenges associated with monitoring tree development in cocoa-growing regions, such as Côte d'Ivoire, the application of this technology within agroforestry and reforestation systems merits investigation. The objective of this study is to evaluate the potential of Airborne Laser Scanning (ALS) for accurate tree height estimation in agroforestry and reforestation systems, thereby enhancing the efficiency of plot-level monitoring. The methodology

integrates drone-mounted LiDAR systems for tree height estimation with floristic and dendrometric field data serving as reference measurements.

2. Materials and methods

2.1. Study area

The study was conducted in West Africa, specifically in the southeastern region of Côte d'Ivoire, within the Agboville Department. The experimental design includes six cocoa-based agroforestry plots and two reforestation plots, located between latitude $06^{\circ}04'$ and $06^{\circ}03'$ north and longitude $04^{\circ}23'$ and $04^{\circ}22'$ west (**Figure 1**). The size of these plots varies between 0.2 and 4.2 ha, with an average of 2 ha (**Table 1**). The reforestation plots are more homogeneous, with a density of 426 trees/ha, while the agroforestry plots are very heterogeneous in terms of tree cover, with a density of 25 trees/hectare. Trees were introduced into these plots in 2020, i.e., these trees are 4 years old, with the presence of a few spontaneous or remanent tree species on both types of plots. All the plots are well maintained, enabling us to carry out this study.

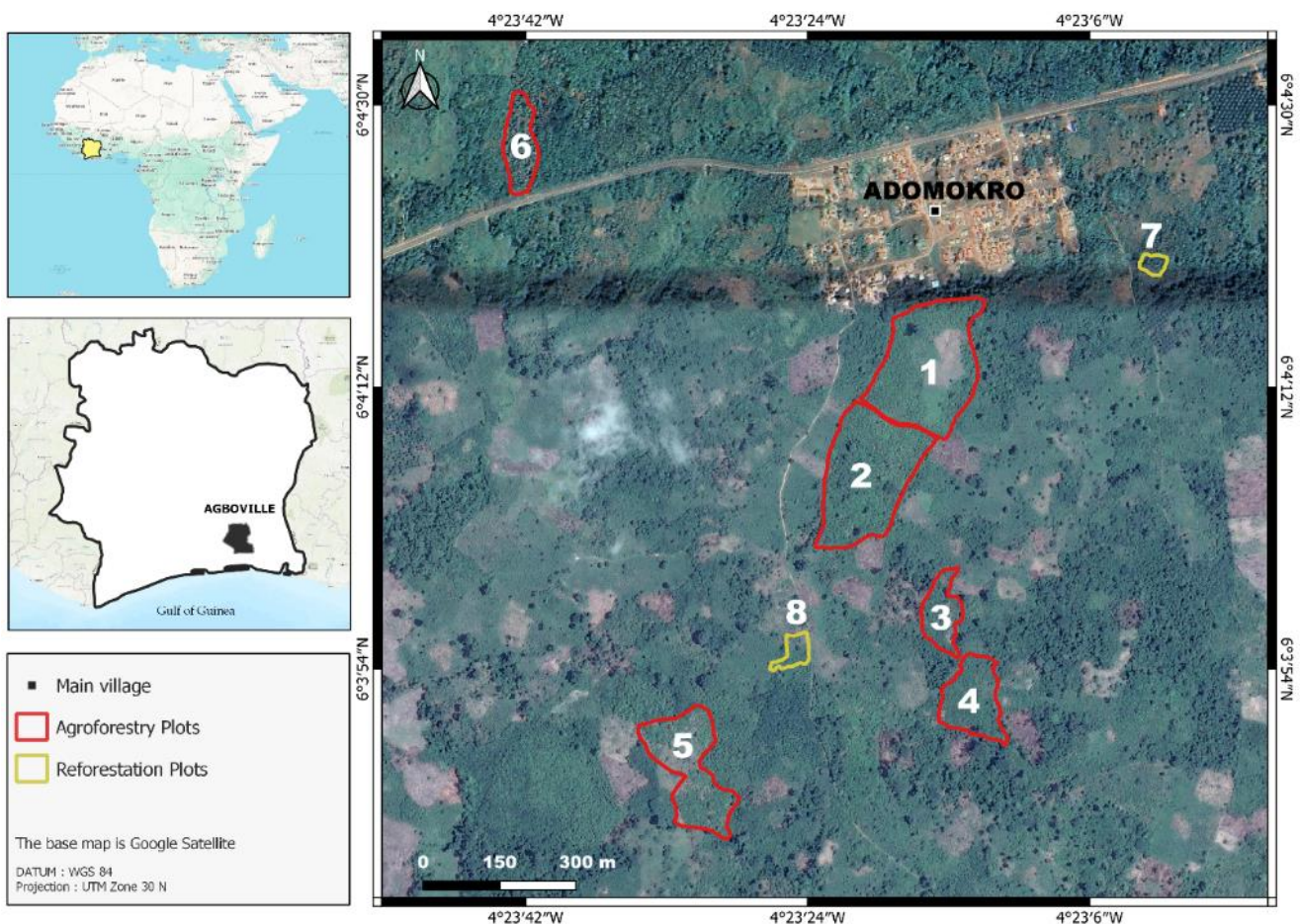


Figure 1. Geographic location of plots. Plots in red are agroforestry plots, and plots in yellow are reforestation plots in the village of Adomokro (Agboville).

Table 1. Characteristics of various plots (UTM Zone 30 N).

Id	Type	Area (ha)	X	Y	Trees planted
1	AGROFORESTRY	4.2	346,391	671,171	
2	AGROFORESTRY	4.0	346,304	670,964	
3	AGROFORESTRY	0.9	346,433	670,695	<i>Terminalia ivorensis</i> , <i>Terminalia Superba</i> , <i>Acacia Mangum</i> ,
4	AGROFORESTRY	1.5	346,498	670,527	<i>Ricinodendron heudoletii</i> ,
5	AGROFORESTRY	2.4	345,942	670,386	<i>Cedrela odorata</i>
6	AGROFORESTRY	1.0	345,613	671,621	
7	REFORESTATION	0.2	346,854	671,379	<i>Terminalia ivorensis</i> , <i>Terminalia Superba</i>
8	REFORESTATION	0.3	346,143	670,622	

2.2. Overall methodology

This section provides a general overview of the steps followed to collect and prepare the data necessary to produce orthophoto, elevation models and their derivatives, and the associated methods. These steps included data collection, data quality check, and processing.

2.2.1. Ground control points marking

Ground control points (GCPs) are points on the ground with known coordinates in the spatial coordinate system (i.e., coordinates defining both horizontal and vertical positions) (**Figure 2**). GCPs were highly beneficial for the ortho-rectification of images and enabled the production of accurate 3D models [16,17]. For GCP collection, their pre-selected locations, based on factors such as terrain, clear grounds, required accuracy, and the nature of the place (either a permanent surface or very short grasses), were proposed. This planning facilitated data collection, as these predetermined points were tracked until the survey crew reached the designated location. After identifying a suitable place for a control point, a mark was placed using a portable ground control point to indicate the center. GCPs were collected using Differential Global Positioning System (DGPS) in the Static observation method to ensure high accuracy, and all the collected points were tied to the Ivory Coast National grid of points using the UTM Zone 30N projected coordinate system. The activity covered the whole 13 plots. The ground control network was established across the DPA to act as horizontal and vertical control during the processing of aerial data. About 15 GCPs were collected in the survey area using DGPS method (**Table 2**).



Figure 2. Sample ground control point (GCP) collected. The central point marked by the cross was collected using Differential Global Positioning System (DGPS) in the static observation method to ensure high accuracy.

Table 2. Table of ground control points (UTM Zone 30 N).

ID	X	Y	Z
GCP1	346,259.0118	671,117.1213	128.7022
GCP2	346,163.0411	670,680.59	138.3985
GCP3	346,081.9614	670,277.0814	127.3008
GCP4	346,522.0614	670,321.5388	129.9778
GCP5	347,042.3994	670,525.8348	117.2303
GCP6	346,428.5486	670,792.4813	134.5087
GCP7	346,810.9346	671,325.6617	126.7313
GCP8	346,377.9837	671,600.1373	122.1037
GCP9	345,766.4521	671,547.3896	120.6868
GCP10	346,165.1991	671,717.85	115.3009
GCP11	346,155.0232	672,492.54	135.8688
GCP12	347,017.4861	672,315.0148	122.545
GCP13	346,751.9487	672,093.5422	127.0172
GCP14	346,981.0794	671,758.2722	137.117
GCP15	347,406.6711	671,980.4339	140.0778

2.2.2. Aerial image acquisition and LiDAR data collection

Both Photogrammetry and LiDAR technologies were used for data collection in aerial surveys, and all those technologies were required at the first step to prepare their flight mission over an area to be surveyed. For Photogrammetry, a high-quality Red-Green-Blue (RGB) camera was mounted on a DJI Mavic 3E to capture many high-resolution photographs over the defined area. The aircraft was flying at 100 m AGL with 80% and 70% forward and lateral overlap, respectively, at an average speed of 6 meters per second. For collecting LiDAR points, the sensor R3 Pro LiDAR (Hesai

Pandar XT32, wavelength: 905 nm, pulse repetition rate: up to 640,000 pulses per second) with 200+ points per square meter was mounted on the designed drone DJI MATRICE M300 RTK to capture 3D points with information useful for generating more precise and accurate elevation models that can rival the accuracy achieved by using conventional ground-based surveys [18]. The flight parameters were readjusted to be able to get enough points that meet the study specifications; the flight height was 80 m AGL, with 80% and 70% as forward and side overlap, respectively (**Table 3**).

Table 3. Table of flight parameters.

Drone	Flight parameters	
	Photogrammetry	LIDAR
	Parameters	
Flight height	100 m AGL	80 m AGL
Forward Overlap	80%	80%
Side Overlap	70%	70%

At the end of each flight mission, a preliminary data quality check in the field was conducted to detect any potential anomalies and to determine whether a re-flight was required.

2.2.3. Data quality check

After each flight, data were checked before sending them to the processing to account for faulty data and assess if a re-flight was required. After a successful quality check, they were sent to the office and backed up to the local storage. At the office, all raw data were imported into the software (Agisoft Metashape 1.8.5) and checked. This was done to assess if the pilots followed the planned route since this could affect data coverage. A thorough check was conducted on the quality of the image, such as lighting, cloud cover, overlap and sidelap, resolution of the imagery, and so forth. If any images failed these checks, this was immediately communicated to re-fly the line. Raw imagery was checked to assess whether there were no cloud covers or shadows. Checks on blurred imagery and lighting were conducted to ensure that the data were good enough to produce high-quality orthophotos. LiDAR point clouds' density was checked. This was required to know if the collected data has enough points to enable analyses of the three-dimensional structure of the vegetation. The average point density was found to be 221.98 points per square meter, and the point spacing was also 0.0671m. In addition to the density of the points, the quality of the points was also checked, as this is the key for registration and georeferencing success.

2.2.4. Floristic and dendrometric data collection

Once the eight plots had been selected, the shapefiles were uploaded to the office GPS. This was followed by an eight-day field mission. The eight plots were covered to collect floristic and dendrometric data. The following indicators were collected on each plot: Geographical coordinates (latitude and longitude) of each tree using a Garmin-type GPS, tree height using a Bosch-type laser rangefinder, Diameters at breast height (DBH) were measured using a tape measure, and botanical identification of tree species on the plots was done. Rangefinder sightings were repeated 4 times to

retain the mean height value. The various variations are due to optical obstacles (branches, foliage, and stems). Once the data had been collected, the information was recorded on physical collection sheets. Trees are marked with a marking spray to avoid double counting. Each evening, the data are downloaded from the GPS using the Dnrgps software, and the data from the collection sheets are entered. After this work, a summary table of the dendrometric measurements of the trees in the plots inspected was set up in Excel, including plot type, tree ID, tree coordinates, species, tree origin, diameter (DBH), and tree height.

2.2.5. Geometric corrections, filtering and ortho-rectified image production

During data processing, the software (Agisoft Metashape 1.8.5) stitches together geotagged drone images with high overlap, captured from multiple angles, and generates an ortho-rectified mosaic image. The steps followed by the software to generate an ortho-rectified image of each plot are shown in **Figure 3**. The steps of point cloud and mesh aim to produce a 3D model and reconstruct an analysis grid to facilitate orthomosaic production. The algorithm used for filtering when generating the dense point cloud is depth filtering. This parameter was moderated for a compromise between density and cloud properties.

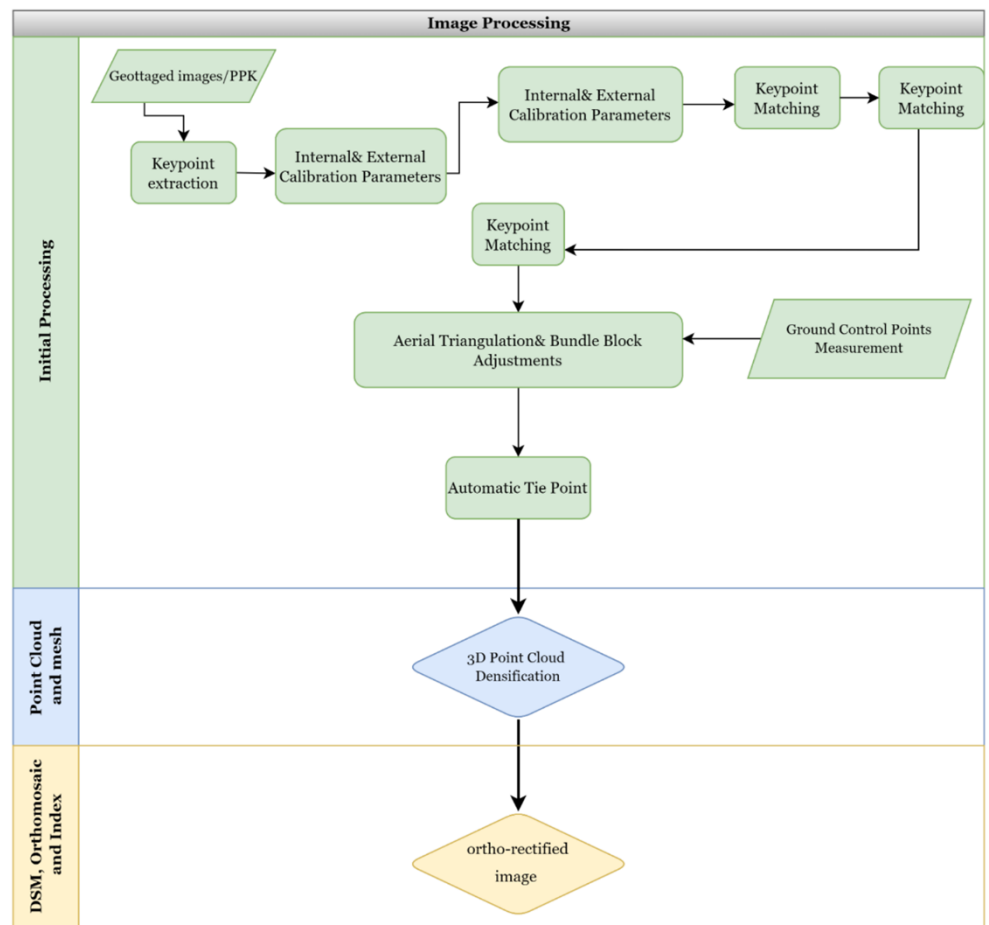


Figure 3. Image processing flowchart to produce Digital Surface Model (DSM) and orthomosaic.

2.2.6. LiDAR point cloud classification and Digital Terrain Model production

Once LiDAR data have been collected, the next step to calculate the individual LiDAR points is often called the “point cloud.” Each laser pulse sent out from the system can have several individual returns. If grass, tree branches, vegetation, power lines, roofs, or any other objects above the ground are struck, a return will be picked up. Often the returns may be in the same position, as can happen when the return comes from bare ground. First, trajectories for each flight were generated and post-processed with Inertial Explorer to get the best fit and accurate aircraft trajectories. The output software then processed the field files and used the post-processed field observations and the feature code to calculate the x , y , and z coordinates of each feature and plot it on the screen as a point. Each flight was processed and calculated individually to ensure the maximum accuracy of the outputs. Then, later various flights were added together into one large project for further processing by generating a LAS point cloud (LASer File format). After obtaining the LiDAR point cloud, it was imported into a point cloud filtering software (CloudCompare 2.6.1) to run the first automatic classification to classify the LiDAR points into ground hits and non-ground hits. This resulted in a greater than 80% correct classification. After the automatic run, a strenuous manual classification was carried out over the required area to edit the points, thus minimizing gross classification errors that may have occurred in the automatic classification process. The output point cloud was then subjected to manual editing and quality assessment to guarantee high-quality elevation models, and the final output from this process was ground points that were later used for Digital Terrain Model (DTM) creation. DTMs are important geodetical products of land surveying [19]. The DTM interpolation method is Triangulated Irregular Network (TIN), which preserves topographic discontinuities.

2.2.7. Ground control points comparison with Digital Terrain Model

The ground control points (GCPs) have been compared to the full LiDAR ground surface and used as a vertical check on the data. On this basis, the Root Mean Square Error (RMSE) was calculated and used to assess the quality of the LiDAR data according to the American Society for Photogrammetry and Remote Sensing reference standards [20].

2.2.8. Canopy Height Model and comparison with ground data

The Canopy Height Model (CHM) was derived by subtracting the DTM from the Digital Surface Model (DSM) [21 – 23]. The trees identified on the ground are then extracted from the CHM to compare the height parameters derived from the photogrammetric and LiDAR data and the data measured in the field with the rangefinder. On this basis, errors were calculated.

3. Results

3.1. Ortho-rectified images and Digital Surface Model

The result was more precise orthophotos of each plot with higher planimetric accuracy and high detail for visualization and decision-making purposes or for other geospatial planning and analyses. The orthorectified images (orthophotos) (**Figure 4**)

of each plot surveyed were provided in Enhanced Compressed Wavelet (ECW) format with an overall high resolution of 0.03 m/pixel. Digital Elevation Model (DSM) (**Figure 4**) captures all the aboveground features, such as vegetation cover and man-made structures, providing a comprehensive representation of what lies on the Earth's surface. This information is crucial for understanding the existing topography and identifying features and their heights, or the variations in their elevation. DSM of each plot surveyed was provided in GeoTIFF format with an overall high resolution of 0.25 m/pixel. This resolution was set to take account of the resolution of the Digital Terrain Model (DTM) and to avoid resampling in the production of the Canopy Height Model (CHM).

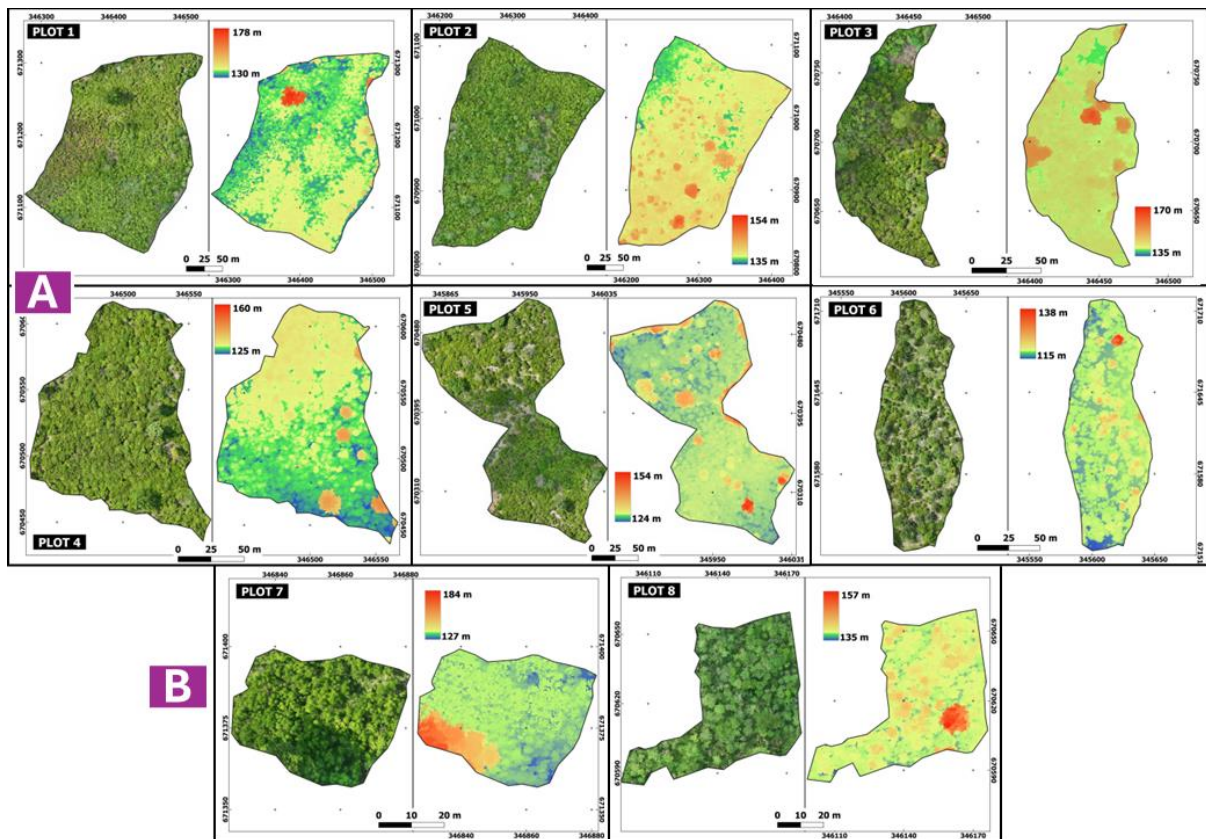


Figure 4. Orthorectified images (orthophoto in the left) and DSMs (in the right) resulting from photogrammetric processing of flights at the 8 plots in March 2024. (A) cocoa-based agroforestry plots and (B) reforestation plots.

3.2. Digital Terrain Model with LiDAR data

The Digital Terrain Model (DTM) generation (**Figure 5**) was done and processed in CloudCompare 2.6.1 and QGIS 3.32 software; LiDAR point clouds were filtered to account for non-ground features and noise points. The target was to remain with only ground points for generating each plot DTM of 0.25 m/pixel with contour lines. The DTM allows for a better appreciation of the topography. In the agroforestry plots, it indicates a topography that varies from 129 m to 134 m in plot 1, representing a difference in level of 5 m. On plot 2, the topography varies from 129 m to 138 m, representing a difference in level of 9 m. On plot 3, the topography varies from 135 m to 138 m, representing a difference in level of 3 m. On plot 4, the topography varies from 124 m to 136 m, representing a difference in level of 12 m. On plot 5, the

topography varies from 123 m to 133 m, representing a difference in level of 10 m. On plot 6, the topography varies from 115 m to 121 m, representing a difference in level of 6 m. In the reforestation plots, on plot 7 the topography varies from 127 m to 129 m, representing a difference in level of 2 m. Finally, plot 8 has a topography varying from 134 m to 139 m, representing a difference in level of 5 m.

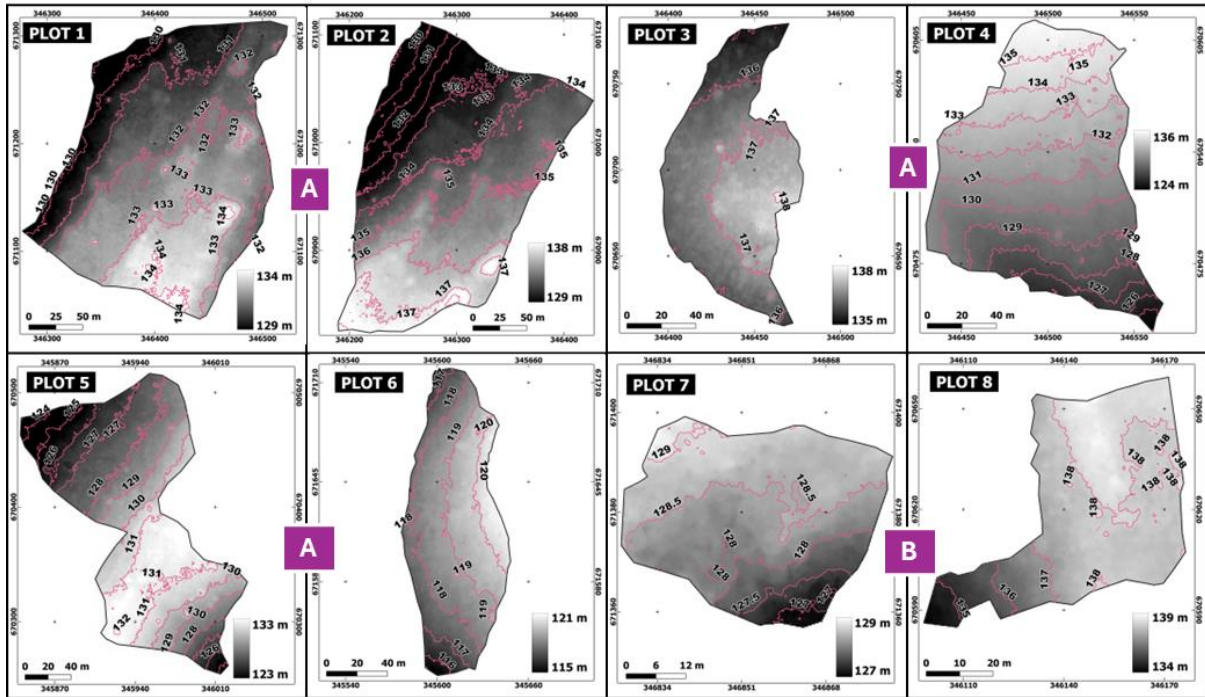


Figure 5. DTMs (contour lines are shown in pink) resulting from LiDAR data processing of flights at the 8 plots in March 2024. (A) cocoa-based agroforestry plots and (B) reforestation plots.

3.3. Canopy Height Model

The Canopy Height Model (**Figure 6**) was derived by subtracting the DTM from the DSM. The CHM resolution is 0.25 m/pixel. The choice of this resolution is justified by the high density of LiDAR points and the need to distinguish individual treetops. This results in a representation of the height of vegetation and structures, offering insights into canopy structure, canopy area, tree height, and variations. CHM is particularly valuable for assessing vegetation health, biomass estimation, and planning agroforestry interventions. On average, reforestation plots contain the largest trees (between 8 and 16 m high), while cocoa-based agroforestry plots contain trees with average heights ranging from 4 to 7 m (**Table 4**).

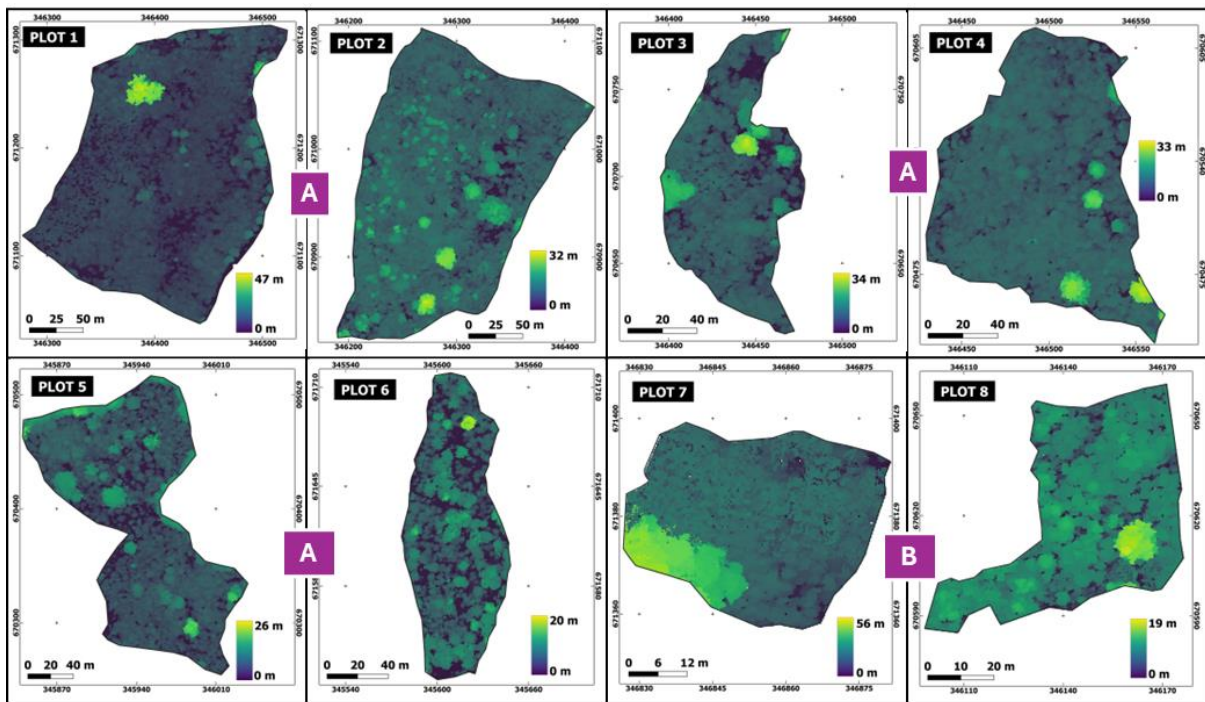


Figure 6. CHMs at the 8 plots. (A) cocoa-based agroforestry plots and (B) reforestation plots.

Table 4. Statistical of Canopy Height Model (CHMs) at each study plot.

Id	Type	Maximum Height (m)	Average (m)	Standard Deviation (m)
1	AGROFORESTRY	46.90	5.47	4.94
2	AGROFORESTRY	32.35	7.34	3.99
3	AGROFORESTRY	33.68	6.84	5.10
4	AGROFORESTRY	32.57	6.80	3.85
5	AGROFORESTRY	26.22	5.86	4.29
6	AGROFORESTRY	19.54	4.04	3.07
7	REFORESTATION	55.88	15.96	10.86
8	REFORESTATION	19.12	7.50	3.14

3.4. Trees extract in Canopy Height Model and comparison with ground inventory data

A total of 506 trees were counted (27 genera and 18 families), measured, and geolocated across the 8 plots studied. These trees were also identified on each of the CHMs to extract the corresponding tree heights (**Figure 7**). Correlation analysis (**Figure 8**) between tree heights measured in the field and those estimated from the CHMs revealed a strong correlation, with a coefficient of determination R^2 of 0.71 (Pearson correlation coefficient $r = 0.84$, p -value = 1.42×10^{-137} , MAE = 1.6722 m, and RMSE = 2.2430 m).

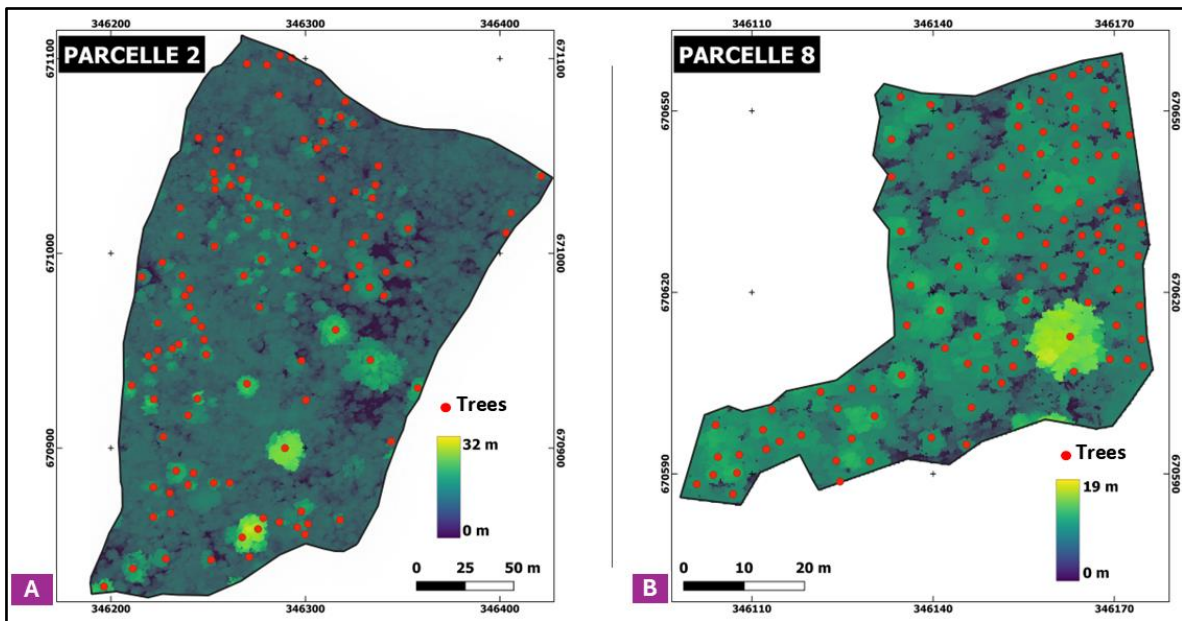


Figure 7. Spatial distribution of trees identified on the CHMs of plots 2 and 8. (A) cocoa-based agroforestry plots and (B) reforestation plots.

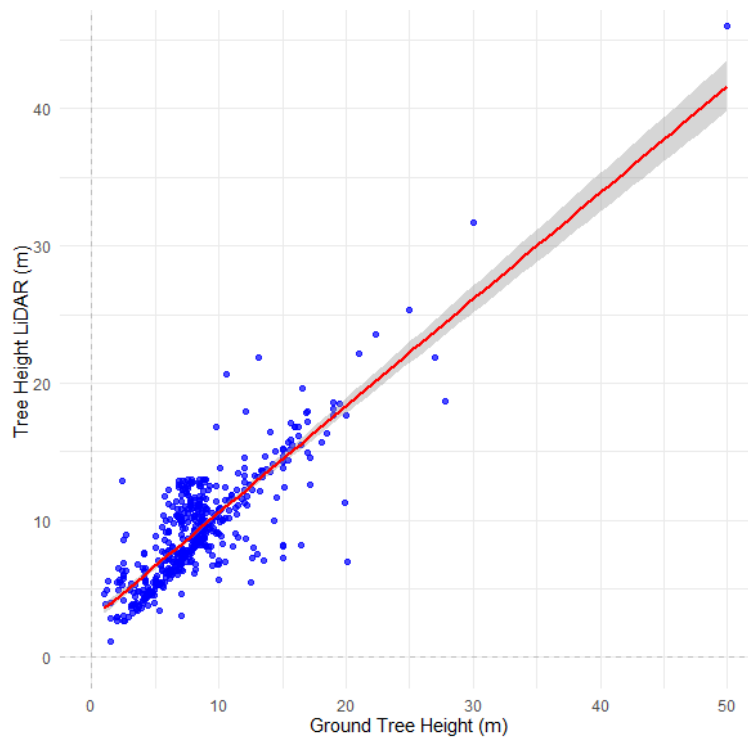


Figure 8. Correlation graph (linear modelling) between tree height measurements obtained with LiDAR technology and tree height measurements inventoried in the field. Regression line (red line) with 95% confidence interval ($R^2 = 0.71$; MAE = 1.67 m; RMSE = 2.24 m).

3.5. Stratified analysis

A stratified analysis shows that the precision of the estimate differs significantly between agroforestry and reforestation plots, given their structural differences. In the agroforestry stratum, on a sample of 293 trees, the errors obtained on this stratum are

much better, with $R^2 = 0.82$; MAE = 1.4336 m; RMSE = 2.2123 m (**Figure 9a**). On the other hand, in the reforestation plots, on a sample of 213 trees, the errors are much greater, with $R^2 = 0.18$; MAE = 1.5208 m; and RMSE = 1.788 m (**Figure 9b**).

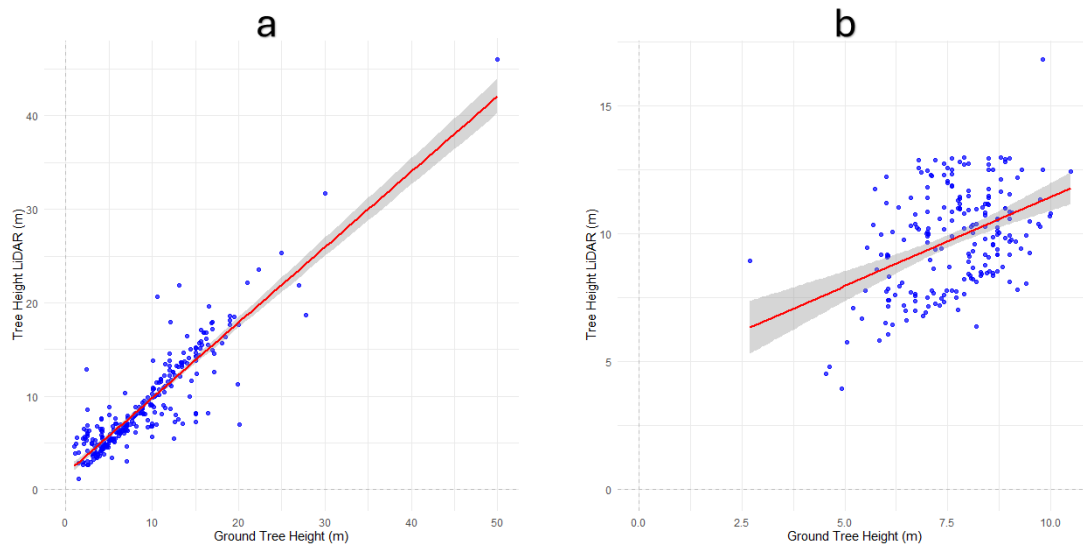


Figure 9. Correlation graph (linear modelling) between tree height measurements obtained with LiDAR technology and tree height measurements inventoried in agroforestry plots (**a**) and reforestation plots (**b**).

4. Discussion

4.1. LiDAR data accuracy and validation with ground data

The methodological approach emphasizes the integration of LiDAR data with ground control points (GCPs) to enhance both planimetric and vertical accuracy, the latter being critical for tree height assessments [21]. Ground control points were compared to the LiDAR-derived ground surface to serve as a vertical validation reference. The final Root Mean Square Error (RMSE) for vertical accuracy was 0.076 m relative to the GCPs, which falls within acceptable thresholds as defined by the American Society for Photogrammetry and Remote Sensing [20]. LiDAR-derived tree heights were further validated against field measurements obtained using a laser rangefinder. The analysis demonstrated a strong correlation, with a coefficient of determination $R^2 = 0.71$ ($r = 0.84$; RMSE = 2.2430 m; MAE = 1.6722 m). These results are aligned with those reported in forest inventory studies by McRoberts et al. [24] and Peterson et al. [25], who also obtained an R^2 of 0.71 in predicting canopy bulk density using airborne LiDAR. Similarly, Kombaté et al. [26] reported a correlation coefficient of $r = 0.84$ for canopy height estimation in savannah forests of Togo using GEDI spaceborne LiDAR. The findings of the present study are also consistent with those of Brou et al. [27], who observed a strong correlation ($R^2 = 0.8$) between drone-derived and field-measured tree heights in cocoa-based agroforestry systems in Côte d'Ivoire, though discrepancies were noted based on tree height and crown class. These results underscore the reliability of the present study's measurements, particularly given the structural complexity inherent to agroforestry environments.

4.2. Source of errors in tree height estimation

Several sources of error may have contributed to the observed RMSE and MAE values. Field measurement inaccuracies, particularly those associated with the use of a rangefinder, include human error, such as misalignment when visually identifying the tree apex, especially under conditions where the crown is partially obscured, and line-of-sight obstructions from branches, foliage, or adjacent stems. O'Beirne [28] highlighted that field-based measurements are prone to higher levels of random error and require labor-intensive procedures, often leading to greater inaccuracies compared to LiDAR-derived estimates. Among the most influential factors affecting field-based error is tree height, which supports the use of LiDAR as a more reliable alternative for such assessments. Another potential source of error lies in tree misidentification, where the tree measured in situ may not correspond precisely to the one detected in the LiDAR dataset due to spatial offset or confusion with neighboring trees [29]. Furthermore, inaccuracies in LiDAR-derived canopy height estimations can arise from orthophoto processing steps, particularly the subtraction of the Digital Terrain Model (DTM) from the Digital Surface Model (DSM), which are sensitive to the interpolation algorithms employed. As noted in prior studies, extracting tree height metrics from LiDAR data in densely forested areas can lead to DTM-related errors, increasing the RMSE by up to 1.95 m [30,31].

4.3. Agroforestry plots vs reforestation plots

Although the trees in this study were all planted in the same year (2020), those in the reforestation plots exhibited greater average heights (ranging from 8 to 16 m) compared to trees in the agroforestry plots, which ranged from 4 to 7 m in height. This difference may be attributed to species-specific responses to environmental conditions, as some tree species are likely better adapted to the open environments typical of reforestation systems than to the more competitive, mixed conditions found in cocoa-based agroforestry. Additionally, the disparity may be linked to differences in management and cultivation practices. Agroforestry systems often involve maintenance activities such as pruning, weeding, and herbicide application to enhance cocoa yield. These interventions can negatively impact the growth and survival of companion tree species [32–34].

This structural heterogeneity between the two systems, in terms of both tree height and density, also affects the accuracy of field-based estimations. Indeed, agroforestry plots yielded more accurate estimates than reforestation plots. The reduced accuracy in the reforestation plots may stem from their high tree density (426 trees/ha) and taller tree heights (8–16 m), which can complicate the visual alignment required for accurate rangefinder measurements. Moreover, dense canopy conditions can introduce errors in Digital Terrain Models (DTMs), thereby increasing the uncertainty in dendrometric parameter estimations [30,31]. These findings are consistent with those of Peng et al. [35], who reported that estimation errors tend to rise with increasing tree height and stand density.

4.4. Challenges in ALS-based dendrometric estimation

This study explored the potential of Airborne Laser Scanning (ALS) for predicting tree diameters. However, several challenges were encountered, particularly in densely vegetated plots. In all study areas, tree density posed a significant constraint to effective detection by automated modeling algorithms. Specifically, reforestation plots had a density of 426 trees per hectare, while agroforestry plots, interspersed with cocoa trees, had a lower density of approximately 25 trees per hectare. Such high-density environments complicate diameter at breast height (DBH) estimation using ALS, especially given that the trees in question generally have small diameters. Manual delineation of tree trunk structures from ALS-derived point clouds proved labor-intensive and challenging under these conditions. While ALS is effective at capturing detailed top-of-canopy structures, it offers limited insight into sub-canopy and trunk architecture due to the scarcity of laser returns from within the canopy [6] (**Figure 10**). This limitation underscores the complementary value of Terrestrial Laser Scanning (TLS) and Mobile Laser Scanning (MLS), which are often used in other studies to provide more complete structural data of forest interiors. Furthermore, a key limitation of the current study is the absence of computer vision techniques, which have demonstrated significant potential for the automated extraction of dendrometric parameters. Recent studies [36 – 39] illustrate how such methods can enhance both the accuracy and efficiency of tree metric estimation from LiDAR data.

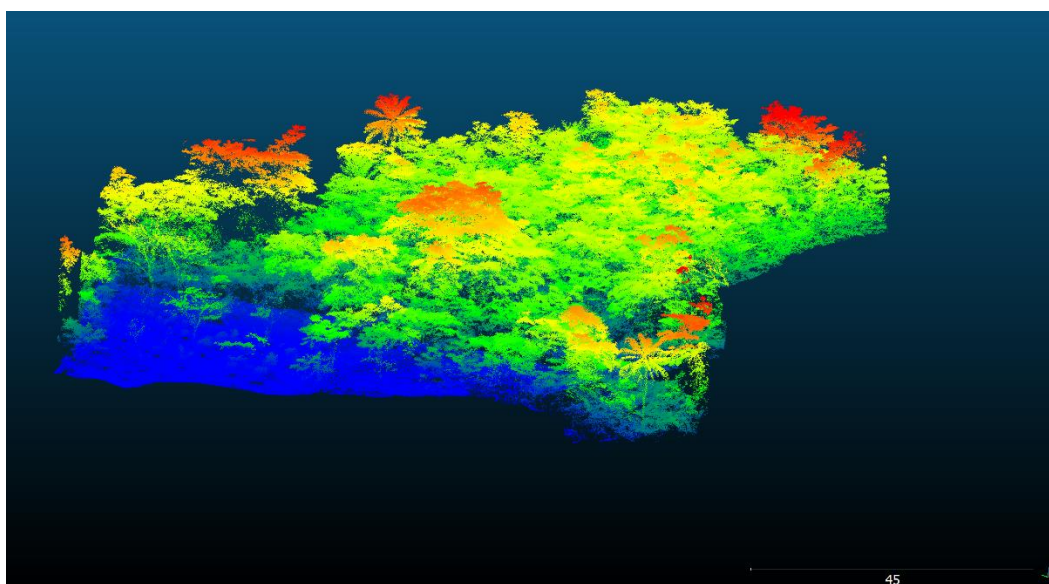


Figure 10. LiDAR point cloud on plot 8 with small, dense trees posing a challenge to estimating tree diameter using automated model algorithms.

5. Conclusions

The objective of this study is to evaluate the potential of Airborne Laser Scanning (ALS) for accurate tree height estimation in agroforestry and reforestation systems, thereby facilitating the monitoring and evaluation of these land-use practices. The methodological framework combined the use of RGB drones and drones equipped with LiDAR sensors to acquire both orthophotos and LiDAR point cloud data across eight study plots. Complementary field surveys were conducted in cocoa-based

agroforestry and reforestation plots to collect floristic and dendrometric data for validation purposes. This study is particularly relevant in the current context of expanding sustainability initiatives, especially agroforestry and reforestation programs, aimed at addressing climate change. As such, there is an increasing need for efficient and accurate monitoring tools to assess tree performance and the effectiveness of these interventions.

The results demonstrated that ALS can reliably estimate tree heights in both systems, with a strong correlation ($R^2 = 0.71$) between LiDAR-derived measurements and field observations obtained using a rangefinder. This level of accuracy was supported by the integration of ground control points (GCPs), yielding a vertical survey accuracy of 0.076 m. The ALS-based approach enabled rapid, safe, and highly accurate data acquisition, offering a clear advantage over traditional ground-based survey methods in terms of time and labor efficiency.

Nevertheless, the study also highlighted limitations in using ALS for estimating tree diameter at breast height (DBH). For more accurate DBH estimation, future studies should explore the application of Terrestrial Laser Scanning (TLS) and Mobile Laser Scanning (MLS) in conjunction with advanced algorithms for cylinder segmentation and trunk detection.

Overall, the findings underscore the value of ALS technology for monitoring agroforestry and reforestation plots and support its integration into the evaluation of sustainability-oriented land management projects.

Author contributions: Conceptualization, TAO, NDK, NG and KKPA; methodology, TAO, NDK, NG, YHME, PM and KKPA; software, TAO, YHME and PM; validation, TAO, YHME, PM and KKPA; formal analysis, TAO, YHME and PM; investigation, TAO, YHME and PM; resources, TAO, YHME, PM and KKPA; data curation, TAO, YHME and PM; writing—original draft preparation, TAO, YHME and PM; writing—review and editing, TAO and YHME; visualization, TAO and YHME; supervision, TAO, NDK, NG, PM and KKPA; project administration, TAO, YHME and PM; funding acquisition, PM and KKPA All authors have read and agreed to the published version of the manuscript.

Acknowledgments: This research was carried out as part of AGROMAP's agroforestry and reforestation project. The authors would like to thank AGROMAP for resources made available for this project. Then CHARIS UAS for providing topographic equipment and technical support to the project team.

Data availability statement: The data of this study are available on this link: <https://doi.org/10.5281/zenodo.15290962>.

Conflict of interest: The authors declare no conflict of interest.

References

1. FAO (Food and Agriculture Organization). Global forest resources assessment 2020: Main report. Food and Agriculture Organization. FAO; 2020.
2. Hansen MC, Potapov PV, Moore R, et al. High-Resolution Global Maps of 21st-Century Forest Cover Change. *Science*. 2013; 342(6160): 850-853. doi: 10.1126/science.1244693

3. SEP-REDD+, FAO. Baseline forest data for REDD+ in Côte d'Ivoire - Mapping forest dynamics from 1986 to 2015 (French). FAO; 2017.
4. Vaudry R, Nourtier M, Bello A, Traoré Y. Qualitative analysis of drivers of deforestation and forest degradation in Côte d'Ivoire (French). Ministry of the Environment and Sustainable Development; 2016.
5. Coffee-Cocoa Council. Guidelines for agroforestry in cocoa production in Côte d'Ivoire (French). Coffee-Cocoa Council; 2023.
6. Dubayah RO, Drake JB. Lidar Remote Sensing for Forestry. *Journal of Forestry*. 2000; 98(6): 44-46. doi: 10.1093/jof/98.6.44
7. Perrin G. Study of forest cover by marked punctual processes [PhD thesis] (French). Centrale Paris Doctoral School; 2006.
8. Doyon F, Sénécal JF, Rochon P. Application of irregular silviculture to hardwood stands deemed unsuitable for gardening. Prediction of gap age and gap type by LiDAR remote sensing in old maple stands. Institut Québécois Forest Management Agency; 2011.
9. Hill J, Lee G, Henry R. Wide-area topographic mapping and applications using airborne light detection and ranging (LIDAR) technology. *Photogrammetric Engineering & Remote Sensing*. 2000; 66(8): 908--914.
10. Dickie S. Application of airborne scanning LIDAR to forestry: Examining stand height and crown closure in annapolis county, Nova Scotia. COGS; 2001.
11. Tarsha Kurdi F, Lewandowicz E, Shan J, et al. Three-Dimensional Modeling and Visualization of Single Tree LiDAR Point Cloud Using Matrixial Form. *IEEE Journal of Selected Topics in Applied Earth Observations and Remote Sensing*. 2024; 17: 3010-3022. doi: 10.1109/jstars.2024.3349549
12. Oliveira PVC, Zhang HK, Zhang X. Estimating Brazilian Amazon Canopy Height Using Landsat Reflectance Products in a Random Forest Model with Lidar as Reference Data. *Remote Sensing*. 2024; 16(14): 2571. doi: 10.3390/rs16142571
13. Ferraz A, Saatchi S, Kellner J, et al. Improving Carbon Estimation of Large Tropical Trees by Linking Airborne Lidar Crown Size to Field Inventory. In: *Proceedings of the IGARSS 2018 - 2018 IEEE International Geoscience and Remote Sensing Symposium*; 2018.
14. Tarsha Kurdi F, Lewandowicz E, Gharineiat Z, et al. Accurate Calculation of Upper Biomass Volume of Single Trees Using Matrixial Representation of LiDAR Data. *Remote Sensing*. 2024; 16(12): 2220. doi: 10.3390/rs16122220
15. Tarsha Kurdi F, Gharineiat Z, Lewandowicz E, et al. Modeling the Geometry of Tree Trunks Using LiDAR Data. *Forests*. 2024; 15(2): 368. doi: 10.3390/f15020368
16. Cevik IC, Atik ME, Duran Z. Investigation of Optimal Ground Control Point Distribution for Geometric Correction of VHR Remote Sensing Imagery. *Journal of the Indian Society of Remote Sensing*. 2024; 52(2): 359-369. doi: 10.1007/s12524-024-01826-0
17. Fitriawan D, Arif DA. A comparison of GNSS measurement methods for orthorectification of high-resolution satellite images: A case study of Worldview-2 and Geoeye-1 satellite images in Padang city, West Sumatera, Indonesia. In: *Advances in geoscience and remote sensing technology*. Springer; 2024.
18. Wulder MA, Bater CW, Coops NC, et al. The role of LiDAR in sustainable forest management. *The Forestry Chronicle*. 2008; 84(6): 807-826. doi: 10.5558/tfc84807-6
19. Štroner M, Urban R, Křemen T, et al. UAV DTM acquisition in a forested area – comparison of low-cost photogrammetry (DJI Zenmuse P1) and LiDAR solutions (DJI Zenmuse L1). *European Journal of Remote Sensing*. 2023; 56(1). doi: 10.1080/22797254.2023.2179942
20. ASPRS. ASPRS Positional Accuracy Standards for Digital Geospatial Data. *Photogrammetric Engineering & Remote Sensing*. 2015; 81(3): 1-26. doi: 10.14358/pers.81.3.a1-a26
21. Lim K, Treitz P, Baldwin K, et al. Lidar remote sensing of biophysical properties of tolerant northern hardwood forests. *Canadian Journal of Remote Sensing*. 2003; 29(5): 658-678. doi: 10.5589/m03-025
22. Piney I. Comparison of Canopy Hole Characterization Protocols on Aerial Photo Time Series: Application to Disturbance Regime Characterization [Master's thesis] (French). Paul Verlaine University of Metz; 2010.
23. Ouattara TA, Sokeng VCJ, Zo-Bi IC, et al. Detection of Forest Tree Losses in Côte d'Ivoire Using Drone Aerial Images. *Drones*. 2022; 6(4): 83. doi: 10.3390/drones6040083
24. McRoberts RE, Reams GA, Van Deusen PC, McWilliams WH. *Proceedings of the seventh annual forest inventory and analysis symposium*. United States Department of Agriculture, Forest Service; 2005.

25. Peterson B, Dubayah R, Hyde P, et al. Use of LIDAR for forest inventory and forest management application. Northern Research Station; 2007.
26. Kombate A, Fotso Kamga GA, Goïta K. Modeling Canopy Height of Forest–Savanna Mosaics in Togo Using ICESat-2 and GEDI Spaceborne LiDAR and Multisource Satellite Data. *Remote Sensing*. 2024; 17(1): 85. doi: 10.3390/rs17010085
27. Brou AL, Akpa L, Kassi J, et al. Drone-based estimation of trees biophysical parameters in complex cocoa-based agroforestry systems. In: *Proceedings of the International Symposium on Cocoa Research 2022 - ISCR 2022*; 2023.
28. Obeirne D. Measuring the urban forest: comparing LiDAR derived tree heights to field measurements [Master's thesis]. San Francisco State University; 2012.
29. Shannon ES, Finley AO, Hayes DJ, et al. Quantifying and correcting geolocation error in spaceborne LiDAR forest canopy observations using high spatial accuracy ALS: A Bayesian model approach. *arxiv*; 2022.
30. Clark ML, Clark DB, Roberts DA. Small-footprint lidar estimation of sub-canopy elevation and tree height in a tropical rain forest landscape. *Remote Sensing of Environment*. 2004; 91(1): 68-89. doi: 10.1016/j.rse.2004.02.008
31. Maguya A, Junttila V, Kauranne T. Algorithm for Extracting Digital Terrain Models under Forest Canopy from Airborne LiDAR Data. *Remote Sensing*. 2014; 6(7): 6524-6548. doi: 10.3390/rs6076524
32. Jagoret P, Michel-Dounias I, Malézieux E. Long-term dynamics of cocoa agroforests: a case study in central Cameroon. *Agroforestry Systems*. 2011; 81(3): 267-278. doi: 10.1007/s10457-010-9368-x
33. Sanial E, Ruf F, Louppe D, et al. Local farmers shape ecosystem service provisioning in West African cocoa agroforests. *Agroforestry Systems*. 2022; 97(3): 401-414. doi: 10.1007/s10457-021-00723-6
34. Kouassi AK, Zo-Bi IC, Aussenac R, et al. The great mistake of plantation programs in cocoa agroforests – Let's bet on natural regeneration to sustainably provide timber wood. *Trees, Forests and People*. 2023; 12: 100386. doi: 10.1016/j.tfp.2023.100386
35. Peng X, Zhao A, Chen Y, et al. Tree Height Measurements in Degraded Tropical Forests Based on UAV-LiDAR Data of Different Point Cloud Densities: A Case Study on *Dacrydium pierrei* in China. *Forests*. 2021; 12(3): 328. doi: 10.3390/f12030328
36. Aijazi A, Checchin P, Malaterre L, et al. Automatic Detection and Parameter Estimation of Trees for Forest Inventory Applications Using 3D Terrestrial LiDAR. *Remote Sensing*. 2017; 9(9): 946. doi: 10.3390/rs9090946
37. Oehmcke S, Li L, Trepekli K, et al. Deep point cloud regression for above-ground forest biomass estimation from airborne LiDAR. *Remote Sensing of Environment*. 2024; 302: 113968. doi: 10.1016/j.rse.2023.113968
38. Xiang B, Wielgosz M, Kontogianni T, et al. Automated forest inventory: analysis of high-density airborne LiDAR point clouds with 3D deep learning. *arxiv*; 2023.
39. Sheng Y, Zhao Q, Wang X, et al. Tree Diameter at Breast Height Extraction Based on Mobile Laser Scanning Point Cloud. *Forests*. 2024; 15(4): 590. doi: 10.3390/f15040590